Journal of Cerebral Blood Flow & Metabolism (2010) 30, 177–186

www.jcbfm.com

In vivo assessment of macrophage CNS infiltration during disruption of the blood–brain barrier with focused ultrasound: a magnetic resonance imaging study

Hao-Li Liu[1,2], Yau-Yau Wai[2,3,7], Po-Hong Hsu[1], Lee-Ang Lyu[1], Jia-Shin Wu[1], Chia-Rui Shen[4], Jin-Chung Chen[5], Tzu-Chen Yen[2,6] and Jiun-Jie Wang[2,3,7]

[1]*Department of Electrical Engineering, Chang-Gung University, Taoyuan, Taiwan;* [2]*Molecular Imaging Center, Chang-Gung Memorial Hospital, Linkou, Taiwan;* [3]*Department of Diagnostic Radiology and Intervention, Chang-Gung Memorial Hospital, Linkou, Taiwan;* [4]*Department of Medical Biotechnology and Laboratory Science, Chang-Gung University, Taoyuan, Taiwan;* [5]*Department of Physiology and Pharmacology, Chang-Gung University, Taoyuan, Taiwan;* [6]*Department of Nuclear Medicine, Chang-Gung Memorial Hospital, Linkou, Taiwan;* [7]*Department of Medical Imaging and Radiological Sciences, Chang-Gung University, Taoyuan, Taiwan*

Focused ultrasound has been discovered to locally and reversibly increase permeability of the blood–brain barrier (BBB). However, inappropriate sonication of the BBB may cause complications, such as hemorrhage and brain tissue damage. Tissue damage may be controlled by selecting optimal sonication parameters. In this study, we sought to investigate the feasibility of labeling cells with superparamagnetic iron oxide particles to assess the inflammatory response during focused-ultrasound-induced BBB opening. We show that infiltration of phagocytes does not occur using optimal parameters of sonication. Taken together, the results of our study support the usefulness and safety of focused-ultrasound-induced BBB opening for enhancing drug delivery to the brain. These findings may have implications for the optimization of sonication parameters.
Journal of Cerebral Blood Flow & Metabolism (2010) **30,** 177–186; doi:10.1038/jcbfm.2009.179; published online 2 September 2009

Keywords: blood–brain barrier disruption; focused ultrasound; inflammation; SPIO-labeled cellular imaging

Introduction

The potential of focused ultrasound to increase the permeability of the blood–brain barrier (BBB) was initially reported more than a decade ago (Mesiwala *et al*, 2002; Vykhodtseva *et al*, 1995). If microbubbles are combined with ultrasound exposure, the effects of ultrasound can be focused to reduce the acoustic intensity required to produce BBB opening (Hynynen *et al*, 2003, 2005, 2006; Kinoshita *et al*, 2006; McDannold *et al*, 2005). This can diminish the risk of tissue damage and make the technique more easily applied through the intact skull (Hynynen *et al*, 2006). Therefore, focused-ultrasound-induced BBB opening is an advantageous technique for drug delivery to the central nervous system (CNS), because the opening is both localized and temporary.

In most previous studies, confirmation of the opening of the BBB was obtained using contrast-enhanced T1-weighted magnetic resonance imaging (MRI). The leakage of gadolinium-based MR contrast agents can be used as an indicator of BBB opening in T1-weighted scans (Hynynen *et al*, 2001, 2003; McDannold *et al*, 2005; Runge *et al*, 1985). In addition, T2*-weighted MRI sequences may be useful for the detection of hemorrhage during focused-ultrasound-induced BBB opening (Liu *et al*, 2008).

Inappropriate sonication is the main cause of complications encountered while using focused-ultrasound-induced BBB opening. Possible mechanisms of brain damage after application of inappropriate sonication include transcytosis, passage through

Correspondence: Dr Jiun-Jie Wang, Department of Medical Imaging and Radiological Sciences, Chang-Gung University, 259 Wen-Hwa 1st Road, Kweishan, Taoyuan, 333, Taiwan.
E-mail: jwang@mail.cgu.edu.tw or
Dr Tzu-Chen Yen, Department of Nuclear Medicine, Chang-Gung Memorial Hospital, 5 Fu-Shin Street, Kueishan, Taoyuan, 333, Taiwan. E-mail: yen1110@adm.cgmh.org.tw
This study was supported by the National Science Council (NSC-95-2221-E-182-034-MY3) and the Chang-Gung Memorial Hospital (CMRPD34022, CMRPD260041).
Received 17 April 2009; revised 3 August 2009; accepted 6 August 2009; published online 2 September 2009

endothelial cell cytoplasmic openings, opening of tight junctions, and free passage through the injured endothelium. (Sheikov *et al*, 2004, 2008). The widespread opening of tight junctions after a high-intensity-focused ultrasound may favor the passage of proteins, chemokines, or blood cells between the vessel lumen and the surrounding brain tissue, resulting in brain hemorrhage and tissue damage (Liu *et al*, 2008). The leakage of proinflammatory molecules and chemokines into the brain milieu may in turn promote macrophage infiltration and homing. McDannold and coworkers initially showed that focused ultrasound exposure for BBB opening may result in erythrocyte extravasations. Occasionally, a mild inflammatory reaction with macrophage infiltration has also been observed (McDannold *et al*, 2005). However, it is unclear whether activated macrophages originate from circulation or from *in situ* microglia. Activated macrophages from circulation, in concert with other immune competent cells, infiltrate the CNS in different neurologic disorders (Nilupul Perera *et al*, 2006; Price *et al*, 2003; Stoll *et al*, 1998), and macrophage tracking by MRI has been applied in several diseases afflicting the CNS.

Superparamagnetic iron oxide (SPIO) nanoparticles are used for intracellular magnetic labeling of cells to monitor cell trafficking by MR imaging. Superparamagnetic iron oxide particles exhibit magnetic moments that align in an applied magnetic field, creating extremely large microscopic field gradients around the particles that de-phase the neighboring proton magnetic moments, thereby reducing the T2* relaxation time. As SPIO particles are phagocytosed by activated macrophages (Dousset *et al*, 1999*a*), brain SPIO-enhanced MRI might be useful for *in vivo* monitoring of immune cell migration into the CNS. This technique may thus allow the identification of diagnostic and prognostic markers *in vivo*. For example, the study of different experimental autoimmune encephalomyelitis models by MRI with SPIO has suggested that disruption of the BBB is the initial key step in the development of inflammatory lesions (Dousset *et al*, 1999*a b*; Linker *et al*, 2006; Rausch *et al*, 2003; Xu *et al*, 1998). Similarly, MRI studies in animal models of tumor, nerve trauma, brain ischemia, and autoimmune neuritis have shown that macrophages are capable of infiltrating the CNS parenchyma (Bendszus and Stoll, 2003; Kleinschnitz *et al*, 2003; Nolte *et al*, 2005; Stoll *et al*, 2004).

The assessment of macrophage CNS infiltration and activity using MRI with SPIO has been previously reported (Dousset *et al*, 2006; Rausch *et al*, 2001; Weissleder *et al*, 1989). In this study, we sought to investigate (1) the feasibility of labeling cells with SPIO particles for assessing the occurrence of an inflammatory response during focused-ultrasound-induced BBB opening, and (2) whether the optimization of sonication parameters can reduce the occurrence of brain macrophage infiltration during BBB disruption (Figure 1).

Table 1 Summary of the experimental results

	Acoustic pressure (MPa)	*Number of sonications*	*Number of animals*
Control animals	1.1	5	5
	2.45	4	
SPIO-laden group	1.1	9	11
	2.45	12	
Total number	—	30	16

SPIO, superparamagnetic iron oxide.

Materials and methods

Preparation of Animals

All animal experiments were approved by our Institutional Animal Experiment Committee. A total of 16 adult male Sprague–Dawley rats were used in this study. The animals were anesthetized using a mixture of ketamine (40 mg/kg) and xylazine (10 mg/kg). A craniotomy was performed 3 days before ultrasound sonications (i.e., 2 days before SPIO injections) to provide a path for the ultrasound beam, and a cranial window ($\sim 1 \times 1\,cm^2$) was made using a high-speed drill. Skull defects were covered with saline-soaked gauze to prevent dehydration until focused ultrasound was applied. The dura was kept intact during craniotomy. As cutting was performed using a bone saw along the edge of the opened region, no scab was left in the ultrasound beam passage to avoid wave interference.

Monocytes were labeled using commercial SPIO nanoparticles (Resovist, Schering AG, Berlin, Germany, carboxydextran-coated, hydrodynamic size: 60 nm). A total of 11 animals received a dose of 15 μmol/kg through the tail vein $\sim$24 h before sonication and MRI scans. The remaining five animals did not receive SPIO and served as controls. A summary of experiments is listed in Table 1.

Ultrasound Generation, Calibration, and Sonication

The experimental protocol is depicted in Figure 2A. A focused ultrasound transducer (Imasonics, Besancon, France; diameter: 60 mm, radius of curvature: 80 mm, frequency: 1.5 MHz) was used to generate a beam of ultrasound energy. An arbitrary function generator (33120A, Agilent, Palo Alto, CA, USA; DS345, Stanford Research Systems, Sunnyvale, CA, USA) was used to generate the driving signal, which was then fed into a radio frequency power amplifier (150A100B, Amplifier Research, Souderton, PA, USA). The ultrasound pressure field and peak ultrasonic pressure were measured and calibrated in an acrylic water tank using a polyvinylidene difluoride-type hydrophone (Onda, Sunnyvale, CA, USA; calibration range: 50 kHz to 20 MHz, diameter: 0.5 mm) mounted on an in-house designed three-dimensional positioning system. The half-maximum pressure amplitude diameter and length of the produced focal spot were 2 and 10 mm, respectively. Measurements of calibrated pressure magnitudes and focal beam dimensions were both conducted in a degassed water-filled tank.

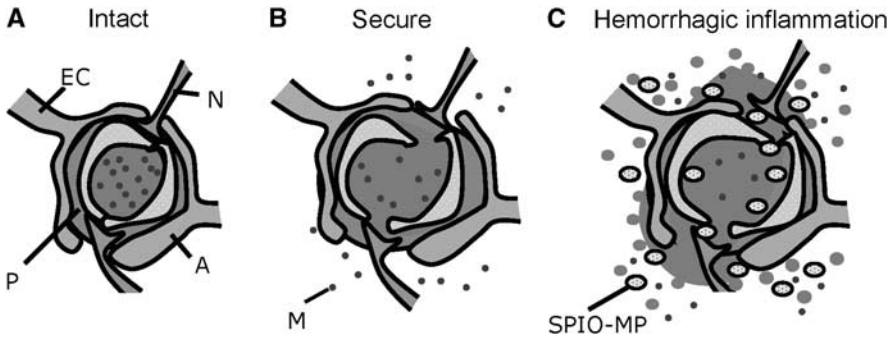

Figure 1 Summary of study hypotheses. (**A**) Cerebral vessels and capillaries with an intact BBB structure; (**B**) secure focused ultrasound sonication induced local and reversible disruption of tight junctions and enhanced the free passage of molecules characterized by a subcellular size; (**C**) stimulation with high-energy ultrasound induced large crafts of the tight junctions and irreversible endothelial damage, resulting in the occurrence of an intracerebral hemorrhage (monitored by heavy T2*-weighted MRI). This in turn induced a significant inflammatory response with macrophage infiltration (monitored by heavy T2*-weighted MRI with SPIO-laden macrophages). EC = endothelial cell, N = neuron, P = pericyte, A = astrocyte, M = subcellular size molecule, SPIO-MP = Superparamagnetic iron oxide nanoparticles (SPIO)-laden macrophage.

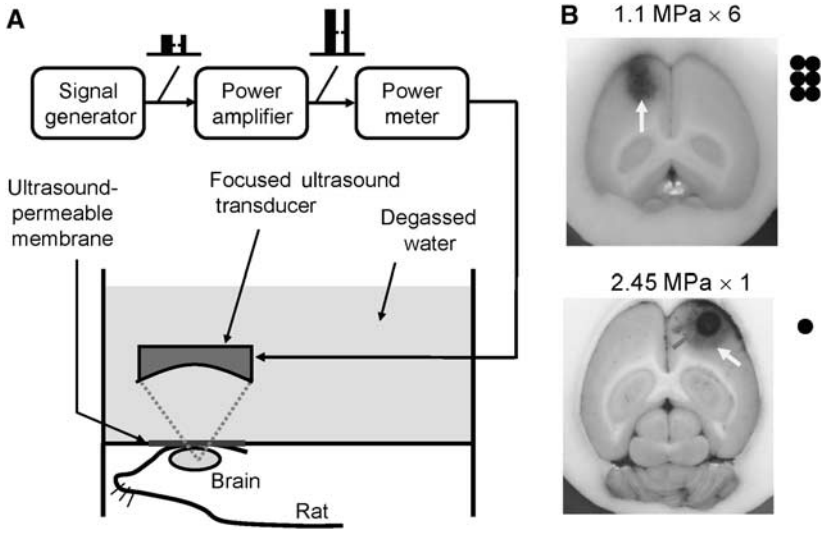

Figure 2 (**A**) Schematic diagram of the focused ultrasound system setup; (**B**) typical blue-dyed brain sections sonicated at 1.1 MPa (resulting in BBB opening) and 2.45 MPa (resulting in BBB opening complicated by intracerebral hemorrhage). Black dots indicate the patterns of sonications used in the two protocols.

A different acrylic water tank with a $4 \times 4\,cm^2$ opening at the bottom was used for animal experiments. To allow the entry of ultrasound, a thin film device was used to seal the opening. Degassed water was filled into the cranial openings to serve as an acoustic coupling device. Animals were placed directly under the water tank with the head tightly attached to the thin-film window.

Ultrasound energy was then delivered into the brain. In the ultrasound exposure experiments, all the brain samples (the only exception being the control tumor group) were sonicated in the presence of an ultrasound microbubble-based contrast agent (sulfur hexafluoride microbubbles 2.0 to 5.0 μm in diameter; SonoVue, Bracco, Milan, Italy) injected intravenously before sonications. Each bolus injection contained 0.025 mL/kg microbubbles ($\sim$0.1 mL/kg, normal adult dose) mixed with 0.2 mL of saline solution and then flushed by 0.2 mL heparin. The center of the focal zone was placed at a 2 to 3 mm penetration depth for each hemisphere. Burst-mode ultrasound was used, with a burst length of 10 msecs, a pulse-repetition frequency of 1 Hz, and a duration of 30 secs. To open the BBB either with or without hemorrhagic damage, we used acoustic negative-peak pressure values (spatial peak and temporal peak) of 2.45 and 1.1 MPa, respectively (the peak values reported in this study have the possibility of being an underestimated value because of the limited resolution of the hydrophone). To achieve a complete opening of the BBB at a low acoustic pressure (1.1 MPa), we performed six different sonications at different points (patterns shown in Figure 2). Microbubbles were injected twice. The first three sonications were conducted consecutively after the first microbubbles injection. The fourth to sixth sonications were conducted after the second microbubbles injection, with at least a 5-min interval between two distinct microbubbles

injections. Sonications were specifically delivered consecutively and unilaterally in the frontal brain, with 1-mm gaps between sonication points. The delay between each sonication was < 5 secs. At high pressure values (2.45 MPa), BBB disruption was easily achieved using a single sonication point. Sonications were performed outside the MRI scanning room.

Magnetic Resonance Imaging

Images were acquired using a 3-T scanner (Trio with Tim, Magnetom, Siemens, Erlangen, Germany) equipped with a homemade surface coil. After sonication, animals placed in an acrylic plastic holder were transferred to the scanning room and then placed inside the bore of the magnet. Contrast-enhanced T1-weighted turbo spin-echo images were obtained as a reference after BBB disruption with the following imaging parameters: TR (repetition time)/TE (echo time) = 534/11 msec, slice thickness = 1.5 mm, matrix size = 134 × 192, field of view = 57 × 83 mm^2, echo train length = 5, and equivalent voxel size = 0.4 × 0.4 × 1.5 mm^3. In all, 10 measurements were acquired in ~5 mins. A dose of 0.25 mL/kg of gadolinium (Gd-diethylene triamine pentaacetic acid (DTPA), Magnevist, Berlex Laboratories, Wayne, NJ, USA) was administered before the image scan, followed by a saline flush solution (0.2 mL/kg) containing 0.2 mL/kg heparin.

Heavy T2*-weighted three-dimensional fast low-angle shot sequences were subsequently acquired for detecting longitudinal changes in the brain parenchyma. Imaging parameters were as follows: TR/TE/flip angle = 28 msec/20 msec/15°, slice thickness = 0.7 mm, number of slices = 16, matrix size = 256 × 384, and field of view = 80 × 130 mm^2, producing a resultant voxel size of 0.3 × 0.3 × 0.7 mm^3, without leaving spaces between adjacent image slices (distance factor = 0%). The image region of interest covered the entire animal brain to achieve a three-dimensional brain reconstruction, as well as for tracking the SPIO-laden macrophages. A total of 5 measurements were acquired in ~7 mins. Animals were continuously imaged within 3 h (at 5-min intervals), as well as at 4 and 24 h. A series of T2* images were acquired at the following time points: (1) 10 mins before sonication, (2) continuously starting from 10 mins after sonication to 3 h after sonication at 10-min intervals, (3) 4 h after sonication, and (4) 24 h after sonication.

Magnetic Resonance Imaging Analysis

To longitudinally monitor slice-based signal intensity (SI) changes from T2* images, the images were first realigned in Matlab (Mathworks, Natric, MA, USA) using a homemade registration algorithm (Dhawan, 2003). Thereafter, regions of interest of 3 × 3 voxels from a single image slide were selected and mean SI values were calculated. Moreover, the volume of hypointense regions in T2* images was calculated using a simple thresholding algorithm (Dhawan, 2003). First, images were linearly interpolated from consecutive slices to a voxel size of 0.3 × 0.3 × 0.35 mm^3 to reduce anisotropy bias in slice direction (i.e., analyzed slices: 31). Images were normalized to the maximum signal intensity of the tissue parenchyma. A binary mask was applied with a threshold of 0.5. Volume was calculated as the sum of pixels in the region of interest multiplied by the known voxel size. Increases in volume were compared in 2.45 MPa sonications either with or without the injection of SPIO particles. The differences in volume increase (observed between 0.5 and 24 h after sonication) were compared using unpaired two-tailed Student's *t*-tests.

Histology

Tissue preparation was performed after *in vivo* MR analysis. Histopathology was performed on 10-μm sections from paraformaldehyde-fixed, paraffin-embedded brain samples. Macrophage infiltration in the brain parenchyma was visualized using the FITC (fluorescein isothiocyanate)-conjugated CD11b mAb (M1/70.15) as described previously (Maruyama *et al*, 2005). For immunocytochemistry, CD11b + peritoneal exudates cells (PECs) in tissue culture dishes were rinsed with phosphate-buffered saline, fixed in 4% paraformaldehyde for 7 mins, rinsed with phosphate-buffered saline, blocked in 2% bovine serum albumin containing 0.1% Triton-X-phosphate-buffered saline, and stained with lymphatic vessel endothelial HA receptor (LYVE)-1 (1:500), podoplanin (1:500), or Prox-1 (1:500). After rinsing and blocking, the samples were subsequently stained with FITC-conjugated CD11b (1:250) secondary antibodies, washed with phosphate-buffered saline, and covered with a Vectorshield with DAPI (4'-6-Diamidino-2-phenylindole) applied for fluorescence. Microscopy was performed using a Zeiss Axiophot microscope (Carl Zeiss Vision, Oberkochen, Germany).

Prussian blue staining (ferric hexacyanoferrate and hydrochloric acid, Sigma, St Louis, MO, USA) was performed to detect focal iron accumulation. Slides were placed in a staining jar containing a hydrochloric acid–potassium ferrocyanide solution for 30 mins at room temperature. The slides were rinsed in distilled water and were counterstained by nuclear fast red for 5 mins. Microscopy was performed using a Zeiss Axioplan 2 imaging microscope with AxioVision 4.1 imaging software, AxioCam HRc camera, and Zeiss objectives Fluar 10 × /0.50, Plan-Apochrome 20 × /0.75, and Plan-Neofluar 100 × /1.30 oil (Carl Zeiss Vision).

Results

As shown in Figure 2B, BBB disruption was obtained using either multiple sonications at an acoustic pressure of 1.1 MPa (upper panel) or a single sonication at the high acoustic pressure of 2.45 MPa (lower panel). Repeated sonications at 1.1 MPa resulted in a larger area of BBB opening compared with that obtained using a single high-pressure sonication (2 mm in diameter at the focal depth). Only few areas of erythrocyte extravasations were evident in regions of BBB opening after sonications at 1.1 MPa. Conversely, a single 2.45-MPa sonication

produced a severe intracerebral hemorrhage (red arrow) within the area of BBB disruption (white arrow).

Figure 3 shows MRI images of control animals and of those receiving SPIO. Gadolinium-enhanced T1 images showed an increase in hyperintense signal at two sites of sonication (left panel: six sonications at 1.1 MPa; right panel: single sonication at 2.45 MPa). Disruption of the BBB was confirmed in both cases. Imaging was continued until 24 h after sonication (i.e., 48 h after SPIO injection in SPIO-treated rats). The T2* image obtained immediately after the T1 image showed hypointensity at the right sonication site. This reflects the presence of an intracerebral hemorrhage due to the excessive acoustic pressure applied during sonication. Notably, the application of six sonications at a pressure of 1.1 MPa did not result in the occurrence of intracerebral hemorrhage. It indicates that this acoustic pressure was relatively safe and below the threshold for hemorrhage.

Subsequent T2* images obtained at 4 and 24 h showed different patterns. The area of hypointensity was specifically relatively constant in the control group, whereas it was significantly expanded in SPIO-treated rats receiving 2.45 MPa sonications. Notably, the signal loss on T2* images caused by intracerebral hemorrhage in animals sonicated at 2.45 MPa showed a consistent hypointense pattern through 24 h.

Figure 4 shows the reconstructed hypointense volume in the same animals used for the experiments reported in Figure 2. The hypointense volume in SPIO-negative rats was found to be rather unchanged (ranging from 0.61 to 0.76 mm^3), whereas an apparent increase was evident in SPIO-treated animals (from

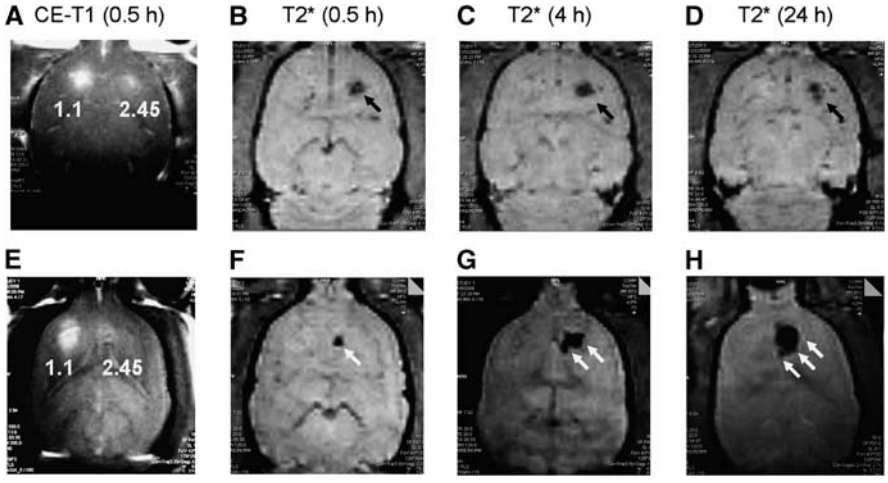

Figure 3 Typical MRI findings of rat brains in animals that either did not receive superparamagnetic iron oxide nanoparticles (upper panel) or were treated with SPIO (lower panel) 24 h before sonication. Images were obtained at different time points, i.e., 0.5 (both CE-T1 (**A**, **E**) and T2* (**B**, **F**)), 4 (T2* (**C**, **G**)), and 24 h (T2* (**D**, **H**)). In each animal, both multiple sonications at 1.1 MPa and a single sonication at 2.45 MPa were used in the left and right forebrain, respectively. In animals sonicated at 2.45 MPa, MRI was able to detect the occurrence of cerebral hemorrhage at 0.5 h through a substantial SI decrease. A similar hemorrhagic pattern persisted for at least 24 h (black arrows). The occurrence of an inflammatory response was evidenced (lower panel) by the continuous expansion of the region, with SI decreased at the site sonicated with a 2.45 MPa pressure (white arrows). This phenomenon was due to the aggregation of SPIO-laden macrophages causing a high image susceptibility effect.

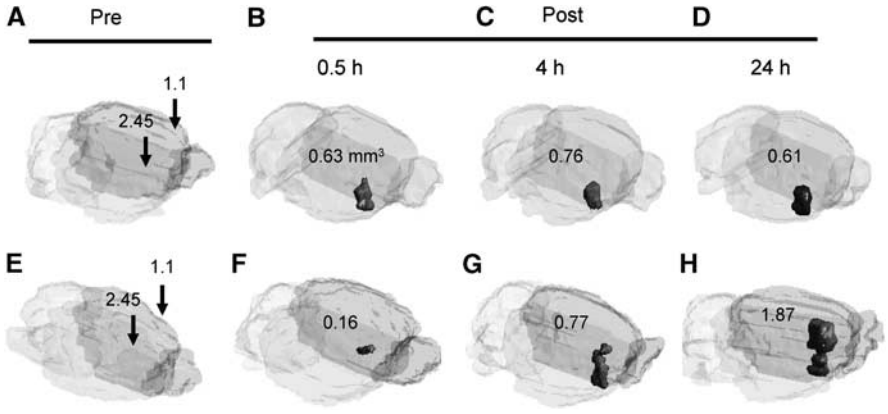

Figure 4 Reconstruction of the hypointense volume presented in Figure 3 from T2*-MRI. (**A**, **E**) Before sonication; (**B**, **F**) 0.5 h after sonication; (**C**, **G**) 4 h after sonication; (**D**, **H**) 24 h after sonication.

0.19 mm^3 at 0.5 h to 1.87 mm^3 at 24 h, a nearly ninefold increase in this case). Figure 5 shows the comparisons of the increases in hypointense volume observed in consecutive T2* images in the control (2.45 MPa) and SPIO-laden (2.45 MPa) groups. The control group showed a homogenous and slight decrease (−10.8% ± 7.3%), whereas the SPIO-laden group showed a heterogeneously increased volume (320.9% ± 246.6%). The differences in volume increase between the two groups were statistically significant ($P = 0.001$).

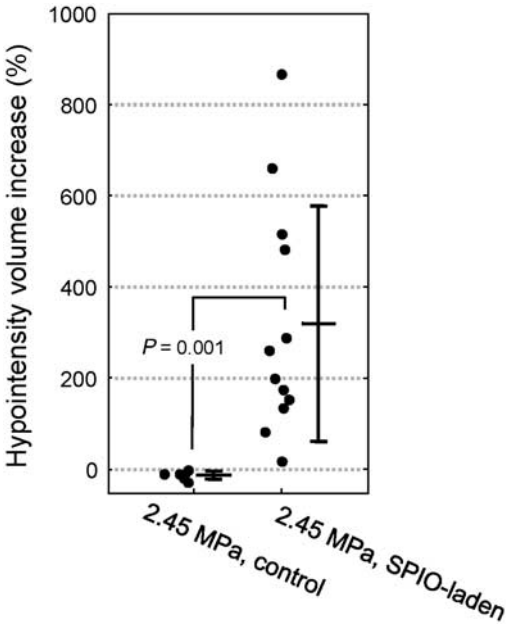

Figure 5 Increase in the hypointense volume in control ($n = 4$) and SPIO-laden ($n = 12$) groups after 2.45-MPa sonications. Data are presented both as individual increases (black dots) and mean ± s.d. (bars). The SPIO-laden group showed a statistically significant increase ($P = 0.001$) in volume (320.9% ± 246.6%) compared with the control group (−10.8% ± 7.3%).

The occurrence of an inflammatory response in areas of BBB opening is also evident in T2* images obtained at 3 h. Figure 4 shows the analysis of MRI SI time course in SPIO-treated animals. Five selected regions are zoomed and depicted (Figure 6A), including blood vessels neighboring the brain (regions 1 and 2), brain areas sonicated at 1.1 and 2.45 MPa (regions 3 and 5), and midbrain artery (region 4). Ultrasonic energy was delivered at 10 mins after the initiation of T2* scans (arrow). Five selected time points are shown in Figure 6B, and the corresponding time changes in SI were recorded accordingly (Figure 6C). As shown in Figure 6, multiple sonications at 1.1 MPa (region 3) did not result in the occurrence of brain hemorrhagic damage, and no apparent signal change was evident. In addition, there was no apparent SPIO-laden monocyte infiltration in these areas. Conversely, a single sonication at 2.45 MPa induced the formation of intracerebral hemorrhage that, in turn, resulted in an immediate 10% signal decrease, followed by another gradual decrease. The total decrease in SI at the end of imaging was 15% at the end of 3 h. These findings suggest a continuous infiltration of SPIO-labeled macrophages at sites sonicated at 2.45 MPa (Figure 3). It is interesting that an ~30% SI decrease was evident in selected neighboring blood vessels. This decrease peaked at ~60 mins and subsequently increased to baseline values. A similar pattern of SI decrease was detected in the midbrain artery (region 4), although to a lesser extent (~12% from baseline values). The pattern in SI changes in circulatory areas (regions 1, 2, and 4) was characterized by a quick SI rebound. This suggests that SPIO-laden macrophages did not stall in these areas. This pattern was therefore different from that observed in areas of suspected inflammation (region 5).

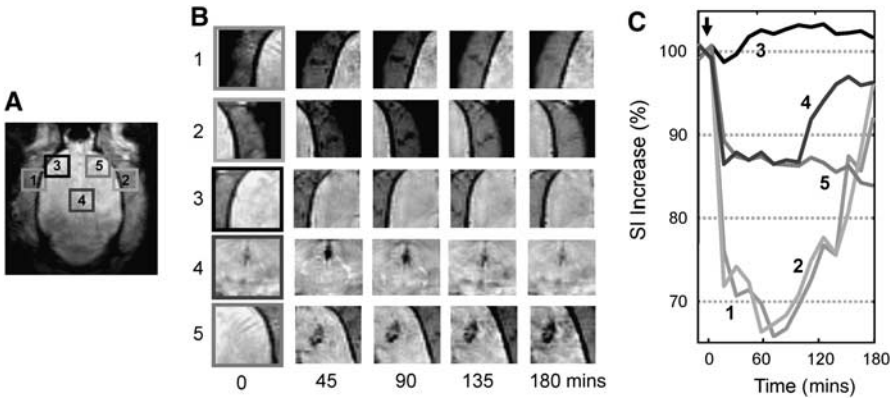

Figure 6 (**A**, **B**) Three-hour longitudinal MRI follow-up imaging of brain regions sonicated at 1.1 and 2.45 MPa. 1 = left-sided blood vessel, 2 = right-sided blood vessel, 3 = sonication site (1.1 MPa), 4 = midbrain artery, and 5 = sonication site (2.45 MPa); (**C**) corresponding changes in MRI signal for regions depicted in panels A and B. In blood vessels and midbrain, SI decreased immediately after sonication and reached a maximal decrease of 30% after 1 h. It subsequently and gradually increased to baseline values at the end of MRI scanning. SI at the site of sonication had a marked initial decrease within the first half hour and subsequently showed a gradual decrease over time. The signal did not recover during the image-monitored session.

Accordingly, inflammatory areas were characterized by a gradual decrease in SI because of infiltration and accumulation of SPIO-laden macrophages.

Superparamagnetic iron oxide-laden macrophages were also confirmed histologically by FITC-conjugated CD-11b immunostaining, as well as by Prussian blue iron staining. Figure 7 compares different focused ultrasound sonication protocols. Specifically, multiple sonications at 1.1 MPa (upper panel), and a single sonication at 2.45 Mpa either without (middle panel) or with (lower panel) an SPIO injection, are depicted. As expected, repeated sonications at 1.1 MPa did not elicit an inflammatory response at irradiated sites. Accordingly, no CD-11b-positive cells were evident. Although some fluorescent-positive cells were evident, they were likely to belong to local microglia. In contrast, areas sonicated at 2.45 MPa showed the presence of CD11b-positive cells (panels E and H), suggesting that sonication with high acoustic pressures was associated with significant macrophage infiltration in the brain parenchyma. Iron deposits as assessed by Prussian blue staining were evident in rats treated with SPIO particles only (panel I versus panel G).

Discussion

In this study, we showed that the brain inflammatory response that accompanies ultrasound-induced BBB

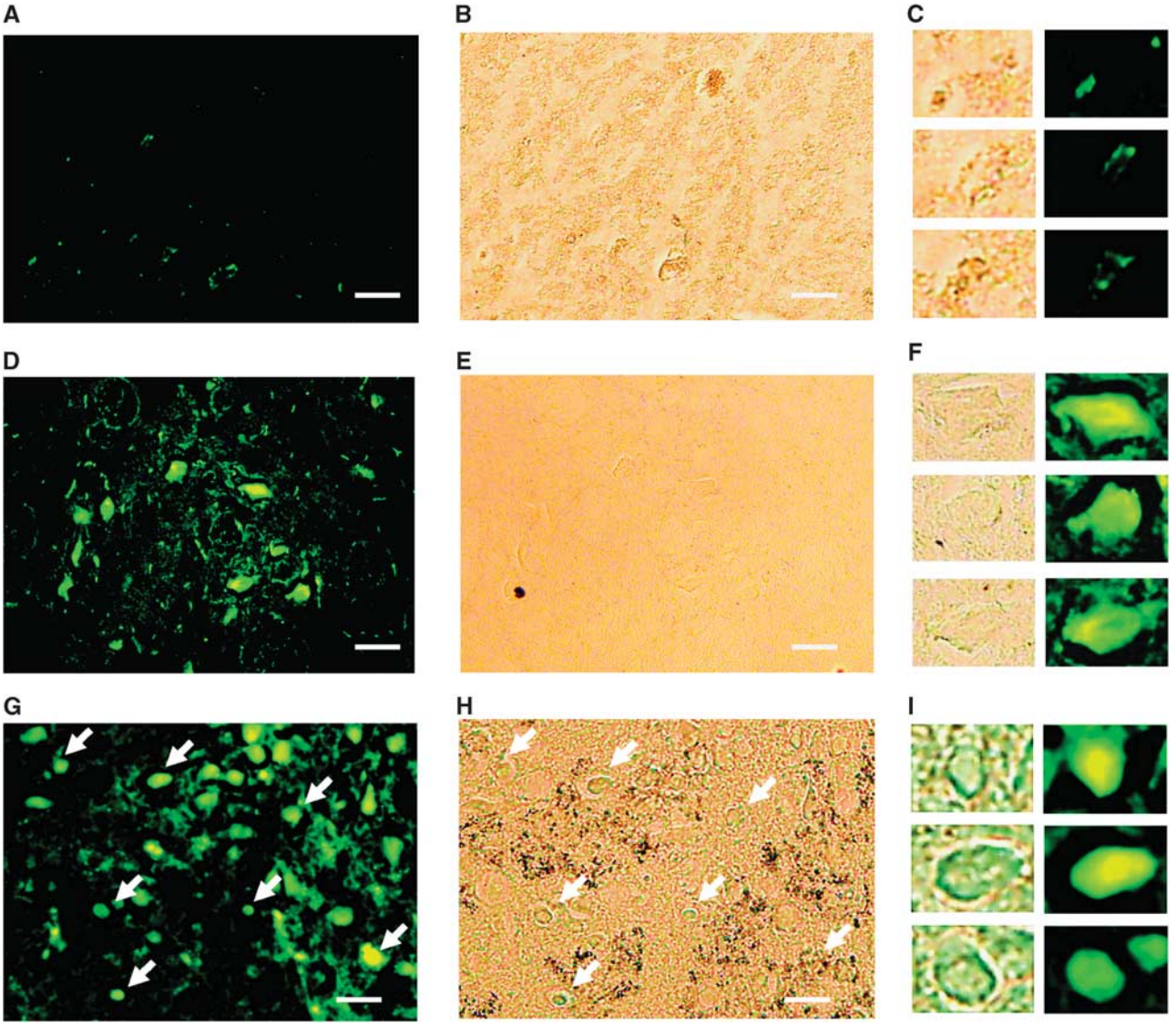

Figure 7 Histological examination to assess the occurrence of an inflammatory response at sites of sonication by FITC-coated CD-11b fluorescent antibodies staining (left panel), Prussian blue staining (middle panel) and the corresponding magnified images (right panel). Row 1 (**A** to **C**): brains sonicated at 1.1 MPa; rows 2 (**D** to **F**) and 3 (**G** to **I**): brains sonicated at 2.45 MPa, either without or with SPIO administration at 24 h before sonication, respectively. Sonications at 2.45 MPa resulted in a significant macrophage infiltration at the site of sonication. Notably, the use of SPIO allowed the tracking of inflammatory response *in vivo* (arrows). Bar = 50 μm.

disruption can be detected using the cell-labeling MRI technique. Our findings may have implications for the optimization of ultrasound parameters.

The phagocytic capacity of activated macrophages and their ability to migrate to inflammation sites have provided the rationale for *in vivo* labeling and monitoring of these cells. The endocytotic loading of circulating macrophages with SPIO has been used in this study to monitor inflammatory response after ultrasound-induced BBB disruption *in vivo* using MRI. The results of our study indicate that a proper selection of sonication parameters can reduce the occurrence of brain macrophage infiltration produced by microbubble-enhanced focused ultrasound stimulation. Our data suggest that hemorrhagic brain damage occurs with the use of high-pressure sonications, resulting in phagocyte infiltration into the brain parenchyma. Intriguingly, the occurrence of an inflammatory response may be avoided using proper sonication parameters.

Temporal Changes in Signal from Blood Vessels

In this study, we showed that superparamagnetic iron oxide MRI can be used successfully to monitor macrophage infiltration into the brain parenchyma after BBB opening by focused ultrasound. The SPIO-laden activity of infiltrating macrophages was characterized by a temporal change in the hypointense pattern detectable both in the damaged brain and in blood vessels. This activity, however, did not originate from signal changes caused by nontargeted SPIO nanoparticles.

Previous studies have consistently shown that the blood pool half-life of SPIO lasts from several minutes (Weissleder *et al*, 1989) to a maximum of 30 mins (Kato *et al*, 1999). After injection of SPIO, the pattern of SI change is characterized by a sharp decrease immediately after SPIO injection, followed by a monotonic increase, and a return to baseline values. In our experiments, SPIO particles were injected into animals 24 h before sonication when no brain damage had occurred. Therefore, the majority of SPIO that was not phagocytosed by macrophages should have been removed from systemic circulation when our sonication experiments were carried out. In addition, we consistently showed that changes in the hypointense pattern were always detectable after 2.45-MPa sonication, but not after 1.1-MPa sonication (data not shown). It is thus unlikely that the temporal signal decrease detected in cerebral blood vessels (Figure 6) could be because of the presence of free SPIO particles in this circulatory territory or because of the effect of gadolinium injection on T2*-weighted image. Moreover, as SPIO was injected before BBB opening, the possibility that changes in hypointensity may be due to the leakage of free-SPIO particles through the disrupted BBB should be excluded. Therefore, we hypothesize that the SI change observed in circulation could be attributed to a transient response of SPIO-laden macrophages recruited into the intracerebral hemorrhage because of high-dose sonication (see regions 1 and 2 in Figure 6).

Time Lapse Selection for Superparamagnetic Iron oxide Injection

The time lapse between intravenous injection and scanning is an important parameter that should be carefully established. This time frame should exceed the blood phase of free contrast agent molecules and should be sufficiently long to allow the accumulation of iron particles within macrophage phagosomes. In this regard, it has been previously shown that all particles had accumulated in macrophages 24 h after intravenous injection, thereby ensuring an optimal use of the macrophage delivery system (Kleinschnitz *et al*, 2003; Weissleder *et al*, 1990).

Focused Ultrasound-Induced Damage

Inappropriate delivery of ultrasonic energy may have undesired side effects. In this regard, several potential complications associated with focused ultrasound-induced BBB opening have been described, including erythrocyte extravasation, microhemorrhage, physical damage of endothelial cells, neuronal damage (hyperchromatic cells, vacuolation), necrotic neuronal death due to excessive acoustic pressure, glial cell neuron pyknosis, or neuron cell apoptosis (Hynynen *et al*, 2005, 2006; Treat *et al*, 2007). Thus far, however, it is still unclear whether such complications are accompanied by an inflammatory response. In this study, we showed for the first time that a significant cellular inflammatory reaction is associated with the occurrence of intracerebral hemorrhage. It is noteworthy that the acoustic pressures used to induce intact BBB disruption or the BBB disruption associated with intracerebral hemorrhage used in this study is in keeping with those previously reported when focused ultrasound was used at a similar frequency (Hynynen *et al*, 2001). Such a response, however, may be the consequence of cerebral hemorrhage and is unlikely to be directly triggered by specific sonication conditions.

Time Course of Inflammatory Response

In recent years, macrophage tracking by MRI with SPIO has been repeatedly used in numerous animal models of CNS diseases. In a rat model of permanent middle cerebral artery occlusion, SPIO was injected intravenously into animals at 5 h, and at days 1, 2, 4, and 7. On T2-weighted images, patch areas of signal loss were evident in infarcted areas until day 4, and were found to be decreased thereafter (Rausch *et al*, 2001). In another model of ischemia (photothrombosis model), the authors reported that *in vivo* labeling of monocytes with SPIO can be confirmed by spatial

agreement with CD11b+ areas, as well as by the incorporation of SPIO nanoparticles into infiltrated monocytes (Saleh *et al*, 2004; Schroeter *et al*, 2004). It is noteworthy that the time course of contrast enhancement has been described to correspond to the time window of monocyte influx (Kleinschnitz *et al*, 2003). In addition, the major wave of macrophage activity was delayed by 5 to 6 days after the induction of cerebral infarcts. Altogether, these findings suggest that the recruitment of hematogenous macrophages occurs similarly in a narrow time interval between days 3 and 6 after the induction of cerebral ischemia.

In this study, we provided evidence that SPIO-laden monocyte activity was evident at the hemorrhagic brain site as early as 4 h after sonication and can be detected early (within 1 h) in the bloodstream. It subsequently increased gradually until 24 h, thereby suggesting that monocyte activity was instantly activated by sonication. This phenomenon could be explained by the fact that focused ultrasound-induced damage is capable of inducing hemorrhagic stroke, but not the ischemic subtype. It is noteworthy that the time course of the inflammatory response in our study was similar to that reported in a previous investigation on intracerebral hemorrhage (Del Bigio *et al*, 1999). Accordingly, these authors showed that intracerebral hemorrhage is accompanied by a significant inflammatory response characterized by immune cell infiltration within 12 h of hematoma onset, with a more marked infiltration of macrophages 1 to 2 days thereafter (Del Bigio *et al*, 1999).

Discrimination Between Microglia and Macrophages

The CNS is characterized by two major monocyte-related populations, i.e., highly ramified resident microglia and hematopoietic perivascular macrophages It is now acknowledged that the CNS does exhibit intense macrophage activity in the early phases of numerous pathologic conditions, including inflammation, demyelination, trauma, or infections (Flaris *et al*, 1993). Resting microglia in the CNS parenchyma are ramified and easily discernible from macrophages. Upon activation, however, microglia undergo morphologic changes and become indistinguishable from hematogenous macrophages on morphologic grounds. The SPIO labeling of resident microglia cells should be ruled out in our study, as the BBB was still intact when SPIO was administered intravenously. We conclude that the pattern of hypointensity observed in longitudinal T2* MRI studies was clearly because of SPIO-laden monocytes and monocyte-derived macrophages.

Acknowledgements

Professor ZH Cho (Neuroscience Research Institute, South Korea) is deeply acknowledged for his support on MRI coil design.

Conflict of interest

The authors declare no conflict of interest.

References

Bendszus M, Stoll G (2003) Caught in the act: in vivo mapping of macrophage infiltration in nerve injury by magnetic resonance imaging. *J Neurosci* 23:10892–6

Del Bigio MR, Yan HJ, Campbell TM, Peeling J (1999) Effect of fucoidan treatment on collagenase-induced intracerebral hemorrhage in rats. *Neurol Res* 21:415–9

Dhawan AP (2003) *Medical Image Analysis*. United States ed., New York: Chichester: Wiley

Dousset V, Ballarino L, Delalande C, Coussemacq M, Canioni P, Petry KG, Caille JM (1999*a*) Comparison of ultrasmall particles of iron oxide (USPIO)-enhanced T2-weighted, conventional T2-weighted, and gadolinium-enhanced T1-weighted MR images in rats with experimental autoimmune encephalomyelitis. *AJNR Am J Neuroradiol* 20:223–7

Dousset V, Delalande C, Ballarino L, Quesson B, Seilhan D, Coussemacq M, Thiaudiere E, Brochet B, Canioni P, Caille JM (1999*b*) In vivo macrophage activity imaging in the central nervous system detected by magnetic resonance. *Magn Reson Med* 41:329–33

Dousset V, Brochet B, Deloire MS, Lagoarde L, Barroso B, Caille JM, Petry KG (2006) MR imaging of relapsing multiple sclerosis patients using ultra-small-particle iron oxide and compared with gadolinium. *AJNR Am J Neuroradiol* 27:1000–5

Flaris NA, Densmore TL, Molleston MC, Hickey WF (1993) Characterization of microglia and macrophages in the central nervous system of rats: definition of the differential expression of molecules using standard and novel monoclonal antibodies in normal CNS and in four models of parenchymal reaction. *Glia* 7:34–40

Hynynen K, McDannold N, Vykhodtseva N, Jolesz FA (2001) Noninvasive MR imaging-guided focal opening of the blood-brain barrier in rabbits. *Radiology* 220:640–6

Hynynen K, McDannold N, Vykhodtseva N, Jolesz FA (2003) Non-invasive opening of BBB by focused ultrasound. *Acta Neurochir Suppl* 86:555–8

Hynynen K, McDannold N, Sheikov NA, Jolesz FA, Vykhodtseva N (2005) Local and reversible blood-brain barrier disruption by noninvasive focused ultrasound at frequencies suitable for trans-skull sonications. *Neuroimage* 24:12–20

Hynynen K, McDannold N, Vykhodtseva N, Raymond S, Weissleder R, Jolesz FA, Sheikov N (2006) Focal disruption of the blood-brain barrier due to 260-kHz ultrasound bursts: a method for molecular imaging and targeted drug delivery. *J Neurosurg* 105:445–54

Kato N, Takahashi M, Tsuji T, Ihara S, Brautigam M, Miyazawa T (1999) Dose-dependency and rate of decay of efficacy of Resovist on MR images in a rat cirrhotic liver model. *Invest Radiol* 34:551–7

Kinoshita M, McDannold N, Jolesz FA, Hynynen K (2006) Targeted delivery of antibodies through the blood-brain barrier by MRI-guided focused ultrasound. *Biochem Biophys Res Commun* 340:1085–90

Kleinschnitz C, Bendszus M, Frank M, Solymosi L, Toyka KV, Stoll G (2003) In vivo monitoring of macrophage infiltration in experimental ischemic brain lesions by

magnetic resonance imaging. *J Cereb Blood Flow Metab* 23:1356–61

Linker RA, Kroner A, Horn T, Gold R, Maurer M, Bendszus M (2006) Iron particle-enhanced visualization of inflammatory central nervous system lesions by high resolution: preliminary data in an animal model. *AJNR Am J Neuroradiol* 27:1225–9

Liu HL, Wai YY, Chen WS, Chen JC, Hsu PH, Wu XY, Huang WC, Yen TC, Wang JJ (2008) Hemorrhage detection during focused-ultrasound induced blood-brain-barrier opening by using susceptibility-weighted magnetic resonance imaging. *Ultrasound Med Biol* 34:598–606

Maruyama II KM, Cursiefen C, Jackson DG, Keino H, Tomita M, Van Rooijen N, Takenaka H, D'Amore PA, Stein-Streilein J, Losordo DW, Streilein JW (2005) Inflammation-induced lymphangiogenesis in the cornea arises from CD11b-positive macrophages. *J Clin Invest* 115:2363–72

McDannold N, Vykhodtseva N, Raymond S, Jolesz FA, Hynynen K (2005) MRI-guided targeted blood-brain barrier disruption with focused ultrasound: histological findings in rabbits. *Ultrasound Med Biol* 31:1527–37

Mesiwala AH, Farrell L, Wenzel HJ, Silbergeld DL, Crum LA, Winn HR, Mourad PD (2002) High-intensity focused ultrasound selectively disrupts the blood-brain barrier in vivo. *Ultrasound Med Biol* 28:389–400

Nilupul Perera M, Ma HK, Arakawa S, Howells DW, Markus R, Rowe CC, Donnan GA (2006) Inflammation following stroke. *J Clin Neurosci* 13:1–8

Nolte I, Vince GH, Maurer M, Herbold C, Goldbrunner R, Solymosi L, Stoll G, Bendszus M (2005) Iron particles enhance visualization of experimental gliomas with high-resolution sonography. *AJNR Am J Neuroradiol* 26:1469–74

Price CJ, Warburton EA, Menon DK (2003) Human cellular inflammation in the pathology of acute cerebral ischaemia. *J Neurol Neurosurg Psychiatry* 74:1476–84

Rausch M, Sauter A, Frohlich J, Neubacher U, Radu EW, Rudin M (2001) Dynamic patterns of USPIO enhancement can be observed in macrophages after ischemic brain damage. *Magn Reson Med* 46:1018–22

Rausch M, Baumann D, Neubacher U, Rudin M (2002) In-vivo visualization of phagocytotic cells in rat brains after transient ischemia by USPIO. *NMR Biomed* 15:278–83

Rausch M, Hiestand P, Baumann D, Cannet C, Rudin M (2003) MRI-based monitoring of inflammation and tissue damage in acute and chronic relapsing EAE. *Magn Reson Med* 50:309–14

Runge VM, Clanton JA, Price AC, Wehr CJ, Herzer WA, Partain CL, James Jr AE. (1985) The use of Gd DTPA as a perfusion agent and marker of blood-brain barrier disruption. *Magn Reson Imaging* 3:43–55

Saleh A, Schroeter M, Jonkmanns C, Hartung HP, Modder U, Jander S (2004) In vivo MRI of brain inflammation in human ischaemic stroke. *Brain* 127:1670–7

Schroeter M, Saleh A, Wiedermann D, Hoehn M, Jander S (2004) Histochemical detection of ultrasmall superparamagnetic iron oxide (USPIO) contrast medium uptake in experimental brain ischemia. *Magn Reson Med* 52:403–6

Sheikov N, McDannold N, Vykhodtseva N, Jolesz F, Hynynen K (2004) Cellular mechanisms of the blood-brain barrier opening induced by ultrasound in presence of microbubbles. *Ultrasound Med Biol* 30:979–89

Sheikov N, McDannold N, Sharma S, Hynynen K (2008) Effect of focused ultrasound applied with an ultrasound contrast agent on the tight junctional integrity of the brain microvascular endothelium. *Ultrasound Med Biol* 34:1093–104

Stoll G, Jander S, Schroeter M (1998) Inflammation and glial responses in ischemic brain lesions. *Prog Neurobiol* 56:149–71

Stoll G, Wesemeier C, Gold R, Solymosi L, Toyka KV, Bendszus M (2004) In vivo monitoring of macrophage infiltration in experimental autoimmune neuritis by magnetic resonance imaging. *J Neuroimmunol* 149:142–6

Treat LH, McDannold N, Vykhodtseva N, Zhang Y, Tam K, Hynynen K (2007) Targeted delivery of doxorubicin to the rat brain at therapeutic levels using MRI-guided focused ultrasound. *Int J Cancer* 121:901–7

Vykhodtseva NI, Hynynen K, Damianou C (1995) Histologic effects of high intensity pulsed ultrasound exposure with subharmonic emission in rabbit brain in vivo. *Ultrasound Med Biol* 21:969–79

Weissleder R, Stark DD, Engelstad BL, Bacon BR, Compton CC, White DL, Jacobs P, Lewis J (1989) Superparamagnetic iron oxide: pharmacokinetics and toxicity. *AJR Am J Roentgenol* 152:167–73

Weissleder R, Elizondo G, Wittenberg J, Rabito CA, Bengele HH, Josephson L (1990) Ultrasmall superparamagnetic iron oxide: characterization of a new class of contrast agents for MR imaging. *Radiology* 175:489–93

Xu S, Jordan EK, Brocke S, Bulte JW, Quigley L, Tresser N, Ostuni JL, Yang Y, McFarland HF, Frank JA (1998) Study of relapsing remitting experimental allergic encephalomyelitis SJL mouse model using MION-46 L enhanced in vivo MRI: early histopathological correlation. *J Neurosci Res* 52:549–58